Journal of Applied Polymer Science

Rheological behavior of polycarbonate/ultrafine octaphenyl silsesquioxane (OPS) composites

Baofa Cheng, Xiangmei Li, Jianwei Hao, Rongjie Yang
School of Material Science and Engineering, Beijing Institute of Technology, National Engineering Research Center of Flame Retardant Material, Beijing 100081, China
Correspondence to: X. Li (E-mail: bjlglxm@bit.edu.cn)

ABSTRACT: Polycarbonate (PC)/ultrafine polyhedral oligomeric octaphenyl silsesquioxane (OPS) composites were prepared by melt mixing method. The morphology and rheological behavior of PC/ultrafine OPS composites were investigated by scanning electron microscopy (SEM) melt indexer, high pressure capillary rheometer, and strain-controlled rheometer. The SEM results show that ultrafine OPS is dispersed in PC as the size of submicron and has a good dispersion in PC matrix, and a certain extent compatibility between PC and ultrafine OPS is found. OPS aggregation is found through the cross section at high ultrafine OPS content. The results of melt flow index (MFI) and capillary rheometer indicate that ultrafine OPS can effectively decrease the apparent viscosity and improve the flow property and processability of PC matrix as a lubricant. The oscillatory rheological analysis indicates that the storage modulus increases with increasing OPS content, and the appeared platform of storage modulus exhibits the solid-like behavior and the formation of three-dimensional network in the composites. The complex viscosity of PC/OPS composite shows a quasi-Newtonian regime at low OPS content and a typical shear-thinning behavior at high OPS content. The Cole–Cole, Han, and van Gurp plots show that ultrafine OPS particle is compatible with PC at low content ($\leq$3 wt %), and interaction between particle and particle is the major factor when OPS at high content ($\geq$6 wt %). © 2016 Wiley Periodicals, Inc. J. Appl. Polym. Sci. **2016**, *133*, 43638.

KEYWORDS: compatibilization; flame retardance; polycarbonates; rheology

Received 4 January 2016; accepted 10 March 2016
DOI: 10.1002/app.43638

INTRODUCTION

Rheological methods have been widely used to study composites incorporated with fillers, since they can detect the presence of internal structures.[1,2] The macroscopic connectivity with three-dimensional network produced from physical interactions can be investigated using rheological methods. Rheological measurement often used to analysis the structure and morphology of polymeric composites, but it extended to study the burning and flame retardant property in recent years. Rheology uses macroscopic testing method to reflect the information of macrostructure, and it is the connection between the microstructure and micro-property. When at a critical loading of filler, the viscoelastic response of the composite system may change from liquid-like to solid-like behavior. Most often, nanoclays, carbon nanofibers/nanotubes, and nanosilica have been the preferred fillers to be used in polymers. However, polyhedral oligomeric silsesquioxanes (POSS) is an organic/inorganic hybrid material, which as new composite has advantages of toughness, good process ability, and both of them have high strength and high temperature resistance. POSS contains a basic polyhedral silicone–oxygen nanostructured skeleton or cage, and the diameter of Si–Si in POSS is precisely defined at 0.53 nm. The incorporation of POSS cages into polymeric materials may result in dramatic improvements in upper use temperature, oxidative resistance, and surface hardening, leading to improved mechanical properties as well as a reduction in flammability. These enhancements have been found to apply to a wide range of thermoplastics and some thermoset systems.[3–5] Although POSS molecules can be thought as the smallest particles of silica, they are physical equivalent in size to most polymer segment.[6,7] Introduction of fillers can affect the morphology and change the rheological behavior of the polymers that filled with nano-sized fillers–filler and matrix interactive forces or polymer chain movement is restricted by filler particles.

Bisphenol A polycarbonate (PC) is one of the most important commercial aromatic polycarbonates, because of its excellent properties, such as transparency, high mechanical strength, good thermal stability, and flame retardancy.[8,9] PC is an amorphous polymer with a relatively high glass transition temperature and viscosity, and it shows a V-2 rate in the UL-94 test. In our previous work, POSS, which are synthesized in this lab as a flame retardant, have been successfully used in PC and make

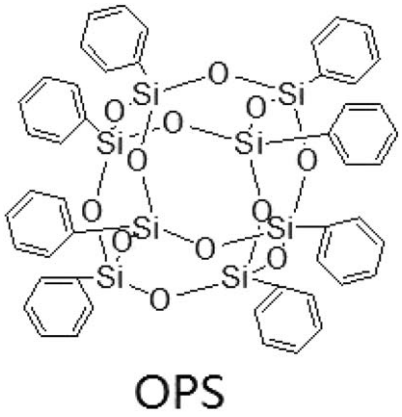

Figure 1. Molecular structure of OPS.

PC has a good flame retardant effect. Ultrafine polyhedral oligomeric octaphenyl silsesquioxane (OPS) at 6 wt % can make PC reach V-0 rating at 1.6 mm and has a good intumescent char residue, and also the addition of OPS can enhance the mechanical properties of PC[10,11]; the ladder polyphenyl silsesquioxane (PPSQ) at 6 wt % can make PC reach V-0 rating at 1.6 mm rating and has a very tall intumescent char residue[12]; and the polyhedral oligomeric silsesquioxane containing 9,10-dihydro-9-oxa-10-phosphaphenanthrene-10-oxide (DOPO-POSS) at 4 wt % can make PC reach V-0 rating at 3.2 mm and has a good intumescent and compact char residue.[11,13] While there have been many studies on the effect of particulate filler of POSS on polymer flame retardancy, there are relatively few studies on the effect of POSS on polymer rheology. In this study, PC/OPS composites were prepared by melting, and the morphology and rheological behavior were analyzed by scanning electron microscopy (SEM), oscillatory measurement, and high pressure capillary rheometer, and we used these measurements were used to study the influence about rheological behavior on flame retardant material of PC/OPS composite.

EXPERIMENTAL

Materials

Makrolon 2805, purchased from Bayer Material science, Leverkusen, Germany. The ultrafine OPS was synthesized by this lab,[6] the schematic representation is shown in Figure 1.

Table I. Composition of Various PC/OPS Composites

Samples	PC content (wt %)	OPS content (wt %)	Antioxygen 168/1010	PTFE
PC	100	0	0/0	0
PC control	99.1	0	0.4/0.2	0.3
1PC/OPS	98.1	1	0.4/0.2	0.3
2PC/OPS	97.1	2	0.4/0.2	0.3
3PC/OPS	96.1	3	0.4/0.2	0.3
6PC/OPS	93.1	6	0.4/0.2	0.3
9PC/OPS	90.1	9	0.4/0.2	0.3

Table II. Processing Conditions of OPS/PC Composites in Twin-Screw Extruder

Barrel zone temp (°C)				Die zone temp (°C)	screw RPM
I	II	III	IV		
245	255	255	255	250	22

Sample Preparation

The composites of PC with different amount of ultrafine OPS (1 wt %, 2 wt %, 3 wt %, 6 wt %, and 9 wt %) were prepared using melt blending method on a twin-screw extruder (SJ-20, diameter $\Phi = 20$ mm; length to diameter L/D=40). The details of OPS content are given in Table I, and the processing conditions of OPS/PC composites are shown in Table II.

Characterization

Melt Flow Index. Melt flow index (MFI) was tested on melt flow indexer, Goettfert Company, Germany, according to ISO1133, load 2.160 kg, the diameter of capillary is 2.1 mm, and test temperature is 290 °C.

Scanning Electron Microscopy. Scanning Electron Microscopy (SEM) experiment was performed with a Hitachi S-4800 scanning electron microscope. The PC/OPS composites were prepared by low temperature liquid nitrogen fracturing and sputtering the cross-section area with gold.

High Pressure Capillary Rheometer. Capillary rheometer test was carried out on a high pressure capillary rheometer RHEOGRAPH 25, Goettfert Company, Germany. The piston diameter was 15.0 mm, and the capillary diameter was 1.0 mm and L/D= 30.0. The apparent shear rates within the range of 500 s^{-1} to 4500 s^{-1}, and the testing temperatures were set at 270 °C, 280 °C, 290 °C, and 300 °C separately.

Oscillatory Rheological. Oscillatory rheological measurement was performed on a strain-controlled rheometer RS300 (Haake Co., March & McLennan Agency, New York) with the dynamic frequency ranging from 0.01 to 100 rad/s at 1 Hz. Plate–plate geometry with plate diameter of 25 mm and a gap of 1.0 mm was set. The used sensor was PP20Ti, then plate–plate was heated up to 290 °C. Samples with a thickness of 1 mm were inserted into the gap. In order to work at an appropriate stress value, the stress scan mode was completed prior to the test. Storage modulus (G′), loss modulus (G″), and complex viscosity (η^*) were measured in the frequency sweep experiments.

RESULTS AND DISCUSSION

Morphology Analysis

In Figure 2, the PC/OPS composites morphology were investigated by SEM, and the magnification is 10.0k. In Figure 2(a), it can be seen that the dispersion of particle size of ultrafine OPS is about from 0.1 μm to 0.2 μm, which shows that OPS can disperse in nano-scale size in PC matrix. From Figure 2(b–d), they show that OPS can also disperse in nano-scale size, but some particles begin to aggregate together into a piece as ultrafine OPS content increase. The range of dispersion size is from 0.1 μm to about 0.5 μm due to the particle aggregation, and some

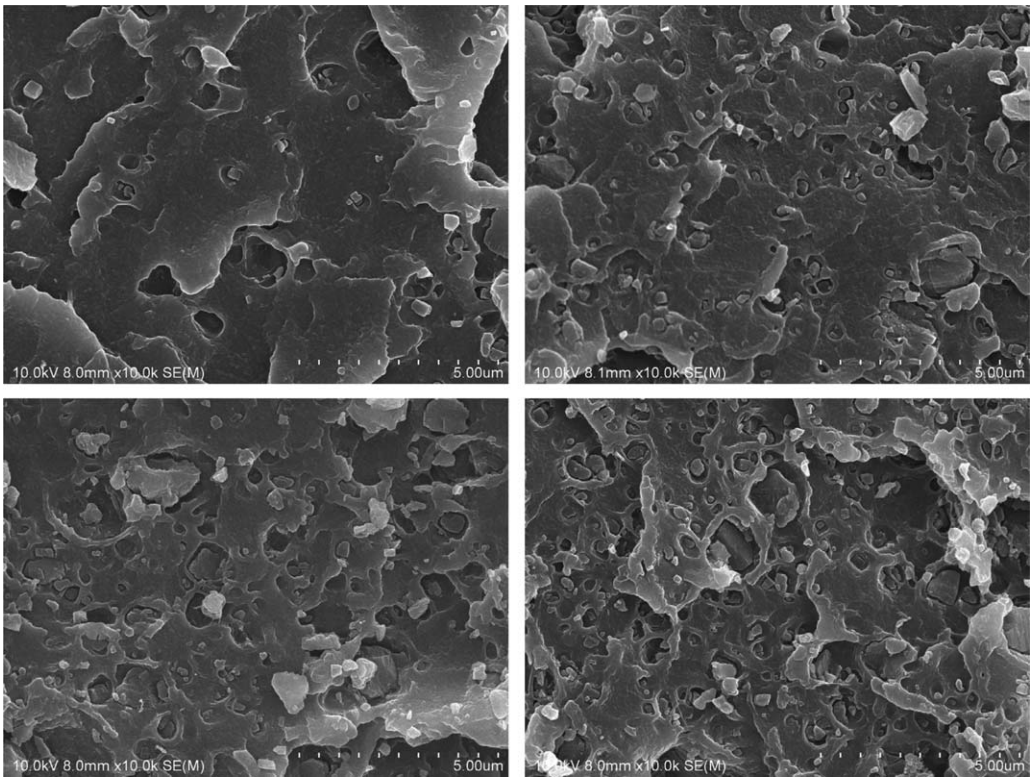

Figure 2. SEM micrographs of PC/OPS composites: (a) 2 wt % OPS; (b) 4 wt % OPS; (c) 6 wt % OPS; and (d) 9 wt % OPS.

big aggregate particles are peeled off from the cross section, but OPS particle also has a good dispersion in PC matrix.

From Figure 2, we can conclude that ultrafine OPS has a good dispersion in PC matrix, and the particle size is close to nano-scale at low OPS content, and big aggregation piece appeared in the cross section, and the aggregation size below 0.5 μm.

Melt Flow Index

The melt flow behavior of PC/OPS composites are illustrated by the melt flow rate (MFR) and melt volume rate (MVR) measurements, which is shown in Figure 3. The value of MFR shown a slight increase at lower OPS content (1–3 wt %), and then presented a sharp increase and reached peak at 6 wt % OPS content, and thereafter decreased with the increasing of OPS content. The result of MVR and MFR indicates that PC/OPS composites as a flame retardant material, the addition of OPS improve the flow ability of PC.

High Pressure Capillary Rheometer

Capillary rheometry is the reference technique for study of the rheological behavior of polymer melts at processing rates. It allows the determination of the material steady-state flow properties by correlating the flow rate imposed with the pressure applied to drive the flow of a polymer melt into a capillary die from a wider space. The piston-drive Goettfert capillary rheometer (Rheograph 15) was used to measure the apparent viscosity at high shear rate. Figure 4 shows the apparent viscosity curve of PC/OPS composites versus apparent shear rate at 270 °C, 280 °C, 290 °C, and 300 °C, respectively. PC control, which contains PTFE and antioxidant, is used to compare with PC.

In Figure 4, it shows that apparent viscosity of PC exhibits a typical shear-thinning behavior of polymer melts-a decrease of viscosity with increasing shear rate during the test; PC control and PC that contain 1–3 wt % OPS also show a shear-thinning behavior, but the amplitude of variation of apparent of viscosity is much smaller than that of PC; PC that contain 6 wt % and 9 wt % OPS show a slight variation of apparent viscosity during the test. At 270 °C, the apparent viscosity of PC control is slight higher than that of PC/OPS composites, but the value of apparent viscosity of PC control is decreased twice compared with that of PC. From 280 °C to 300 °C, the apparent viscosity of

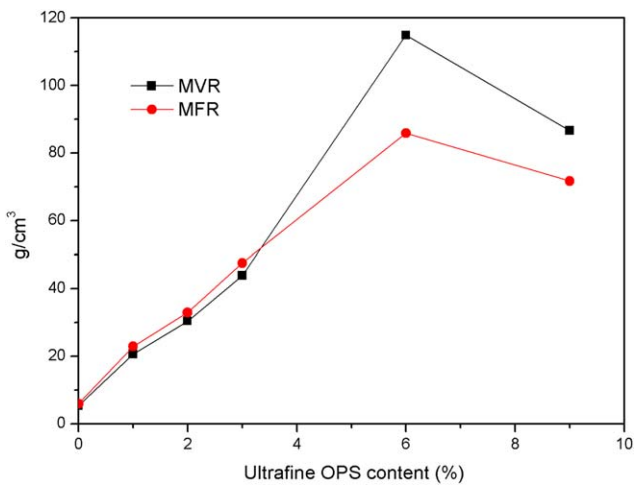

Figure 3. MVR and MFR of PC/OPS composites. [Color figure can be viewed in the online issue, which is available at wileyonlinelibrary.com.]

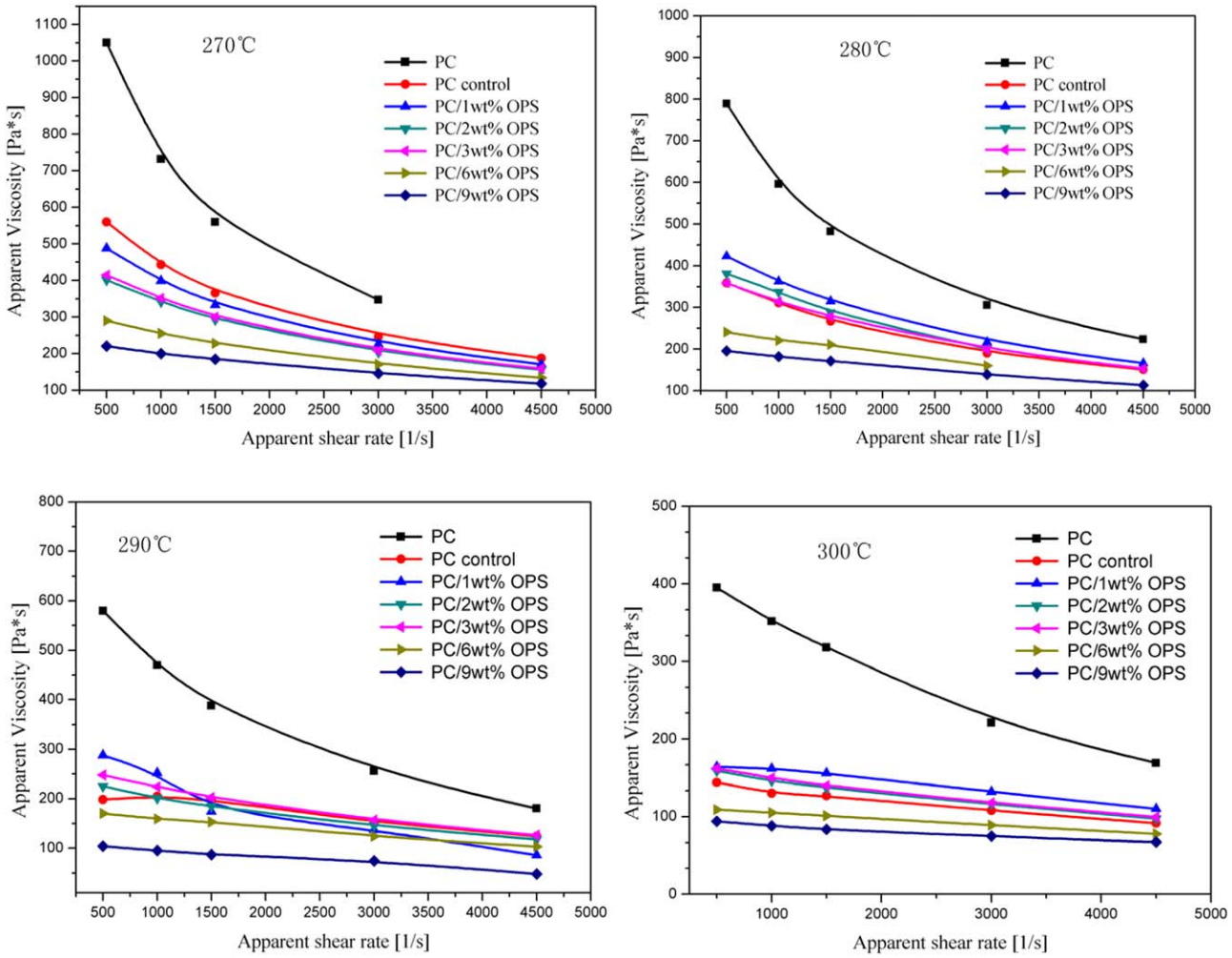

Figure 4. Apparent viscosity of PC/OPS composites versus apparent shear rate. [Color figure can be viewed in the online issue, which is available at wileyonlinelibrary.com.]

PC is lower than that of PC that contain 1–3 wt % OPS, but higher than 6 wt % and 9 wt % OPS content of PC/OPS composites. At 290 °C and 300 °C, the apparent viscosity of PC/OPS composites has slightly variation with apparent rate increase.

In Figure 4, it can be seen that the compatible at low ultrafine OPS content leads to a fine dispersion between PC chain and OPS interaction according to the results of SEM analysis of PC/OPS composites, which is weak van der Waals forces. This interaction could probably cause decreased chain entanglements and supply more free volume in the melt as the ultrafine OPS acts as a lubricant of PC, thus lead to decrease the viscosity of PC during the process.

Oscillatory Rheological Analysis

For viscoelasticity of polymer melt, it can be divided into three measurements, which contain steady state measurement, transient measurement, and dynamic measurement according to the movement of time dependence. The measurement of dynamic viscoelasticity is used for studying the microstructure information of polymer melt. The oscillatory rheological analysis was used to study the microstructure of PC/OPS composites. In Figures 5 and 6, they present the variation of G′, and η^* with frequency between PC and PC/OPS composite. Through the results of apparent viscosity of PC and PC/OPS composites, the testing temperature for oscillatory rheological test is 290 °C.

In Figure 5, the curve shows that the storage modulus (G′) of PC/OPS composite is increased with the ultrafine OPS content increasing at low angular frequency. In Figure 5, it can be seen that the slope of G′ vs. ω (oscillatory angular frequency) is gradually becoming smaller as the ultrafine OPS content increasing compared with PC. When OPS content exceeds 3 wt %, it can be seen that a platform appeared which means G′ does not change with the frequency at low angular frequency region. According to the formula $G' \propto \omega^2$ (where ω is the oscillatory angular frequency) at terminal region of low frequency, PC and PC/OPS composites present a typical liquid-like characteristic at low OPS content (1–2 wt %). It was reported that solid-like behavior had been observed in conventional filled polymer systems in which there were existing strong interactions among the polymers and the fillers.[14] When ultrafine OPS content exceeds 6 wt %, the slope is so low that it forms a G′ platform zone which indicates the OPS particle control the relaxation behavior of composites, and PC/OPS composites from a liquid-like behavior transfer to a solid-like behavior which means a

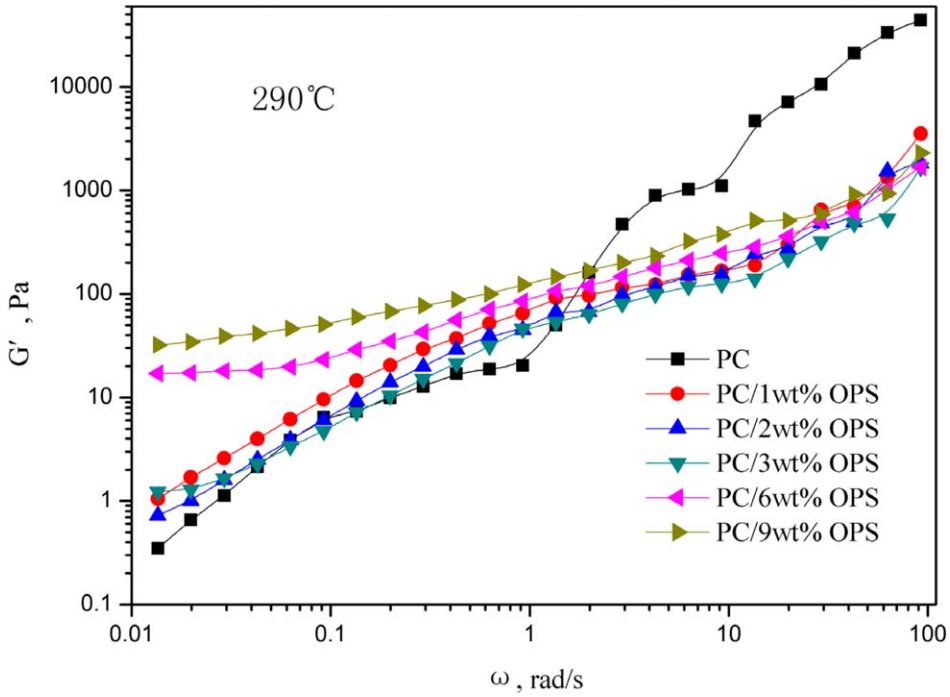

Figure 5. Storage modulus of PC/OPS composites. [Color figure can be viewed in the online issue, which is available at wileyonlinelibrary.com.]

three-dimensional network appeared in PC/OPS composite. For PC/OPS composites, this three dimensional network is helpful to from a compact and strong char during the combustion, which have a good flame retardant effect for material.[10,11]

The complex viscosity (η^*) of PC and PC/OPS are showing in Figure 6. It presents that at 1 wt % and 2 wt % ultrafine OPS content, PC/OPS composites exhibit quasi-Newtonian fluids with slight viscosity variations during the test. When the ultrafine OPS exceed 3 wt %, the PC/OPS composites exhibit a typical shear-thinning behavior of polymer melt. At low frequency region, the η^* of PC/OPS composites present a tendency that η^* reduce at the initial and then increased as the ultrafine OPS content increase, and η^* of PC/OPS composites are higher than PC when OPS exceed 6 wt %. When polymer filled with particles, the composite will be more show an obvious shear-thinning behavior if the filler

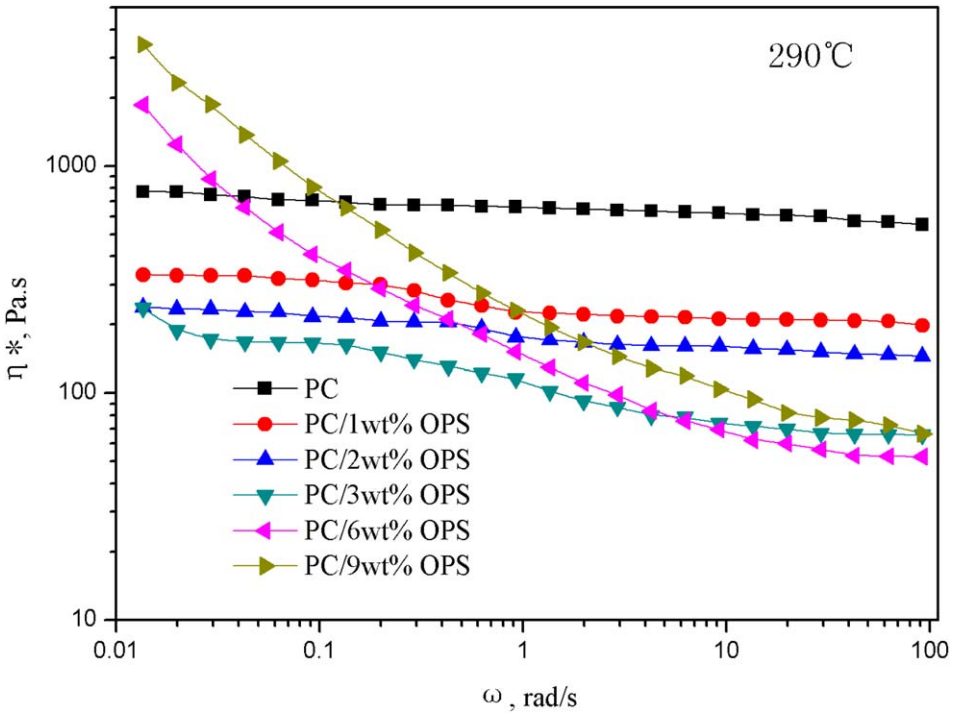

Figure 6. Complex viscosities of PC/OPS composites. [Color figure can be viewed in the online issue, which is available at wileyonlinelibrary.com.]

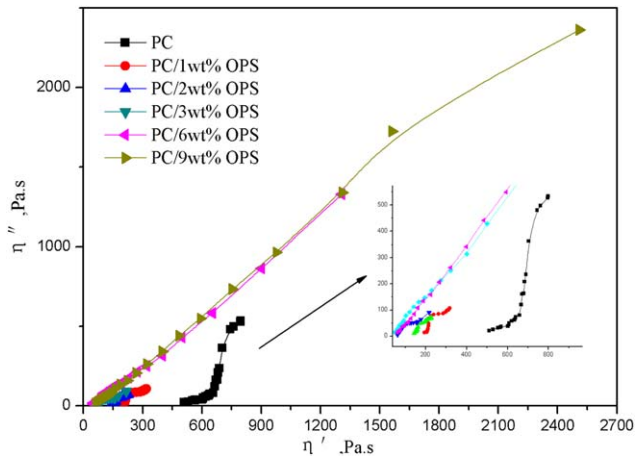

Figure 7. Cole–Cole plots of PC/OPS composites. [Color figure can be viewed in the online issue, which is available at wileyonlinelibrary.com.]

content exceed a critical value as the fill increase, and the G′ will be obviously increased at low frequency region and even a platform is appeared.[15,16] This is in accordance with Figure 5.

From Figures 5 and 6, it can be concluded that the addition of ultrafine OPS improve the G′ of PC at low angular frequency, and the appearance of the platform indicates that a three dimensional network formed in the PC/OPS composites. The η^* of PC/OPS composite is higher than that of PC, it due to the particle aggregation which hinder the flow and thus raise the viscosity, which is accordance with MFI results, and all these results are useful for forming a compact and strength char residue.[10–13]

The Cole–Cole and Han Analysis of Rheological Behavior

The Cole–Cole plot is used to exhibit the relationship between the real part (η') and the imaginary part (η'') of complex viscosity. It have been reported that the plot can be used to describe the viscoelasticity of distribution of relaxation time characteristic of heterogeneous polymer material and analyze the miscibility of polymer blend, and the curve can also reflect the existing network structure.[17,18]

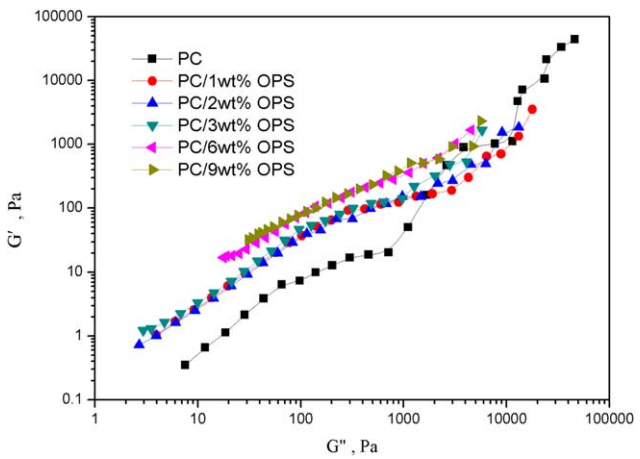

Figure 8. Han plots of PC/OPS composites. [Color figure can be viewed in the online issue, which is available at wileyonlinelibrary.com.]

The theoretical basis of Cole–Cole plot is Maxwell model. It is appropriate for describing the simple system of relaxation laws.[19–21] A smooth, semicircular shape of the plotted curves would suggest good compatibility, i.e., phase homogeneity in the melt, and any deviation from this shape shows a nonhomogeneous dispersion and phase segregation due to immiscibility.[22–24]

The Cole–Cole plots of PC/OPS composite shows in Figure 7. In Figure 7, it can be seen that the shapes of composites with 1, 2, and 3 wt % ultrafine OPS are close to an arc-shaped, and a smooth, semicircle shape of the plotted curve would suggest good compatibility (or at least finely dispersed), which indicates that ultrafine OPS could have a good dispersion in PC matrix at low content. When the content of ultrafine OPS reach 6 wt % and 9 wt %, the Cole–Cole plot of PC/OPS composites are significantly deviated from the arc-shaped and show more evident up turning at high viscosity at high OPS content, which the results are in accordance with Figure 6. This deviation is probably due to the strong anchor effect of OPS in PC matrix, and this phenomenon reflects the incompatibility relationship with the existing three-dimensional structure in the composite. Therefore, we can conclude that OPS have a good dispersion in PC and exists certain compatibility between PC and OPS at low content of OPS.

Figure 8 shows the Han plot of PC/OPS composites. The Han plot has been widely used to investigate compatibility and effect of polydispersity in polymer blends.[25,26] Han plot is independent of the melt temperature and weight-average-molecular weight for mono-dispersed polymer. In Figure 8, it shows that the Han plot of PC/OPS composites deviated largely from the scaling G″–G′ of the linear polymer at high ultrafine OPS content (more than 6 wt %), which indicates that a long relaxation time occurred in these samples. The result exhibits that above 6 wt % ultrafine OPS content, the composites behave in an anomalous way and a phase separation of OPS and PC has occurred. Unlike the deviation for composite at high OPS content, the OPS would be good dispersed in PC matrix because of the compatibility at low OPS content. These results are consistent with Cole–Cole plot.

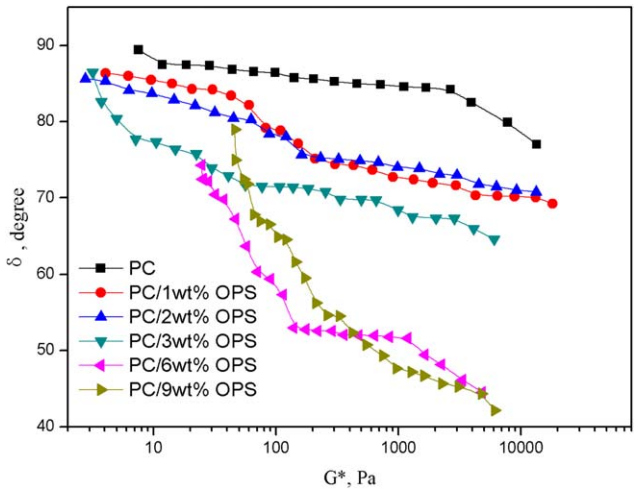

Figure 9. Van Gurp's plot of PC/OPS composites. [Color figure can be viewed in the online issue, which is available at wileyonlinelibrary.com.]

Van Gurp Analysis

The van Gurp plot representing the relationship between the complex modulus and delta is used to the verification of the time temperature superposition principle,[27] miscibility of polymer blends,[28] and rheological percolation of polymer composites.[29] Figure 9 shows the van Gurp plot of PC/OPS composites. It can be seen that the curve variation tendencies are similar to the neat PC and PC/OPS composites at 1 wt %, 2 wt %, and 3 wt % ultrafine OPS content, but the deviation were particularly notable for 6 wt % and 9 wt % ultrafine OPS of PC/OPS composites. According to Reichert,[30] the deviation indicates that interfacial has changed in the melt during the experiment. The different rheological behaviors of POSS/polymer composites melt could be attributed to two factors: the interaction between the POSS aggregates (particle–particle interaction), and the interactions between the POSS and the polymer matrix. The particle–particle interaction is the major factor for physical blending composites. [6,31] For the physical blending composites of PC/OPS, the slightly deviation of Cole–Cole plot and van Gurp plot at high ultrafine OPS content (≥6 wt %) indicates that the particle–particle interaction is main factor, which is so weak that the deviation only occurs at high ultrafine OPS content.

CONCLUSIONS

Flame-retarded polycarbonate (PC) composites have been obtained by incorporation of an ultrafine polyhedral oligomeric octaphenyl silsesquioxane (OPS). The ultrafine OPS were dispersed with submicron particle size in PC matrix at low OPS content, and particle size became bigger due to the particle aggregation effect at high OPS content. OPS improved the flow and processability of PC by high pressure capillary, and could decrease the apparent viscosity and apparent press during the processing. The storage modulus of PC/OPS was much higher than PC, especially at high OPS content (≥6 wt %). When OPS content exceeded 6 wt %, a platform zone appeared at low angular frequency, which mean PC/OPS composites from a liquid-like state transfer to solid-like state. The variation of complex viscosity of PC/OPS composites results showed that PC and PC/OPS composites exhibited a quasi-Newtonian fluid when OPS content below 3 wt %, and showed a typical shear-thinning behavior when OPS content exceeded 3 wt %. Cole–Cole plot, Han plot, and van Gurp analysis results indicated that OPS particles had a good dispersion and a certain compatible in PC at low content.

ACKNOWLEDGMENTS

This research was received the financial support from the National Natural Science Foundation of China, Youth Science Found project (No. 51303011) and Basic Research Foundation of Beijing Institute of Technology (No. 20130942002).

REFERENCES

1. Horst, R. H.; Winter, H. H. *Macromolecules* **2000**, *33*, 130.
2. Pogodina, N. V.; Lavrenko, V. P.; Srinivas, S.; Winter, H. H. *Polymer* **2001**, *42*, 9031.
3. Joshi, M.; Butola, B. S. *J. Macromol. Sci.* **2004**, *C44*, 389.
4. Liu, L.; Hu, Y.; Song, L.; Nazare, S.; He, S. Q.; Hull, R. *J. Mater. Sci.* **2007**, *42*, 4325.
5. He, Q. L.; Song, L.; Hu, Y.; Zhou, S. *J. Mater. Sci.* **2009**, *44*, 1308.
6. Fu, B. X.; Gelfer, M. Y.; Hsiao, B. S.; Phillips, S.; Viers, B.; Blanski, R.; Ruth, P. *Polymer* **2003**, *44*, 1499.
7. Levchik, S. V.; Weil, E. D. *Polym. Int.* **2005**, *54*, 981.
8. Phillips, S. H.; Haddad, T. S.; Tomczak, S. J. *Curr. Opin. Solid State Mater. Sci.* **2004**, *8*, 21.
9. Joshi, M.; Botola, B. S. *J. Macromol. Sci. Polym. Rev.* **2004**, *44*, 389.
10. Li, L. M.; Li, X. M.; Yang, R. J. *J. Appl. Polym. Sci.* **2012**, *124*(5), 3807.
11. Cheng, B. F.; Zhang, W. C.; Li, X. M.; Yang, R. *J. Appl. Polym. Sci.* **2014**, *131*, DOI: 10.1002/app.39892.
12. Jiang, Y. Y.; Li, X. M.; Yang, R. J. *J. Appl. Polym. Sci.* **2012**, *124*, 4381.
13. Zhang, W. C.; Li, X. M.; Yang, R. J. *J. Appl. Polym. Sci.* **2012**, *124*, 1848.
14. Agarwal, S.; Salovey, R. *Polym. Eng. Sci.* **1995**, *35*, 1241.
15. Soong, S. Y.; Cohen, R. E.; Boyce, M. C.; Mulliken, A. D. *Macromolecules* **2006**, *39*, 2900.
16. Soong, S. Y.; Cohen, R. E.; Boyce, M. C. *Polymer* **2007**, *28*, 1410.
17. Kovacs, J.; Dominkovics, Z.; Voros, G.; Pukánszky, B. *Macromol. Symp.* **2008**, *267*, 47.
18. Wu, D. F.; Wu, L.; Sun, Y. R.; Zhang, M. *J. Polym. Sci. B: Polym. Phys.* **2007**, *45*, 3137.
19. Cao, Q.; Yu, L.; Zheng, L. Q.; Li, G. Z.; Ding, Y. H.; Xiao, J. H. *Colloid Surface A: Physicochem. Eng. Aspect* **2008**, *312*(1): 32.
20. Chopra, D.; Kontopoulou, M.; Vlassopoulos, D.; Hatzikiriakos, S. G. *Rheol. Acta* **2002**, *41*, 10.
21. Tian, J. H.; Yu, W.; Zhou, C. X. *Polymer* **2006**, *47*, 7962.
22. Cho, K.; Lee, B. H.; Hwang, K. M.; Lee, H.; Choe, S. *Polym. Eng. Sci.* **1998**, *38*, 1969.
23. Kim, H. K.; Rana, D.; Kwag, H.; Choe, S. *Korea Polym. J.* **2001**, *8*, 34.
24. Kwag, H.; Rana, D.; Choe, K.; Rhee, J.; Woo, T.; Lee, B. H.; Choe, S. *Polym. Eng. Sci.* **2000**, *40*, 1672.
25. Chuang, H. K.; Han, C. D. *J. Appl. Polym. Sci.* **1984**, *29*, 2205.
26. Han, C. D.; Chuang, H. K. *J. Appl. Polym. Sci.* **1985**, *30*, 4431.
27. van Gurp, M.; Palmen, J. *Rheol. Bull.* **1998**, *67*, 5.
28. Carrot, C.; Mbarek, S.; Jaziri, M.; Chalamet, Y. *Macromol. Mater. Eng.* **2007**, *292*, 693.
29. Mahmoud, A. G.; Pötschke, P.; Zhou, D. H.; Mark, J. E.; Heinrich, G. *J. Macromol. Sci. Pure Appl. Chem.* **2007**, *44*, 591.
30. Reichert, P.; Hoffmann, B.; Bock, T.; Thomann, R.; Mülhaupt, R.; Friedrich, C. *Rapid Commun.* **2001**, *22*, 519.
31. Joshi, M.; Butola, B. S.; Simon, G.; Kukaleva, N. *Macromolecules* **2006**, *39*(5), 1839.